Anti-Cancer Potential of Copper-NTB Complex via Damaging Cellular Organelles and Apoptosis in Triple-Negative Breast Cancer Therapy

Downloaded from: https://research.chalmers.se, 2026-07-17 07:56 UTC

Citation for the original published paper (version of record):
Balusamy, S., Balamurugan, M., Nag, S. et al (2025). Anti-Cancer Potential of Copper-NTB Complex via Damaging Cellular Organelles and Apoptosis in Triple-Negative Breast Cancer Therapy. NANO SELECT, 6(12).
http://dx.doi.org/10.1002/nano.70049

N.B. When citing this work, cite the original published paper.

research.chalmers.se offers the possibility of retrieving research publications produced at Chalmers University of Technology. It covers all kind of research output: articles, dissertations, conference papers, reports etc. since 2004. research.chalmers.se is administrated and maintained by Chalmers Library

(article starts on next page)

Nano Select

RESEARCH ARTICLE OPEN ACCESS

Anti-Cancer Potential of Copper-NTB Complex via Damaging Cellular Organelles and Apoptosis in Triple-Negative Breast Cancer Therapy

Sri Renukadevi Balusamy[1] | Mani Balamurugan[2] | Sagnik Nag[3] | Sourav Mohanto[4] | Mohamed Farouk Elsadek[5] | Nojood Altwaijry[5] | Daewon Sohn[6] | Ivan Mijakovic[7,8] | Priyanka Singh[8] | Haribalan Perumalsamy[9,10]

[1]Department of Food Science and Biotechnology, Sejong University, Seoul, Republic of Korea | [2]Department of Materials Science and Engineering, Seoul National University (SNU), Seoul, Republic of Korea | [3]Jeffrey Cheah School of Medicine and Health Sciences, Monash University Malaysia, Selangor, Malaysia | [4]Department of Pharmaceutics, Yenepoya Pharmacy College & Research Centre, Yenepoya (Deemed to Be University), Mangalore, India | [5]Department of Chemistry, College of Natural Sciences, Hanyang University, Seoul, Republic of Korea | [6]Department of Biochemistry, College of Science, King Saud University, Riyadh, Saudi Arabia | [7]Systems and Synthetic Biology Division, Department of Life Sciences, Chalmers University of Technology, Gothenburg, Sweden | [8]The Novo Nordisk Foundation, Center For Biosustainability, Technical University of Denmark, Kongens Lyngby, Denmark | [9]Research Institute for Convergence of Basic Science, Hanyang University, Seoul, Republic of Korea | [10]Center For Creative Convergence Education, Hanyang University, Seoul, Republic of Korea

Correspondence: Ivan Mijakovic (ivan.mijakovic@chalmers.se) | Priyanka Singh (prisin@biosustain.dtu.dk) | Haribalan Perumalsamy (harijai2004@gmail.com)

Received: 13 March 2025 | **Revised:** 21 July 2025 | **Accepted:** 21 July 2025

Funding: The authors would like to extend their sincere appreciation for funding of this work through the National Research Foundation of Korea (NRF), Grant number: 2020R1A6A1A06046728; Ongoing Research Funding program (ORF-2025-349), King Saud University, Riyadh, Saudi Arabia; NNF Grant number: NNF20CC0035580; and DFF and Thematic Research-Independent green research (2023): 3164-00026A. Sourav Mohanto would like to acknowledge Yenepoya (Deemed to be University), India, for providing the fellowship.
[Correction added on 16 August 2025, after first online publication: Funding information has been updated in this version].

Keywords: Anti-cancer activity | Apoptosis | Breast cancer | Copper | MDA-MB-231 cells | Triple-negative breast cancer

ABSTRACT

Triple-negative breast cancer (TNBC) is a heterogeneous and one of the most common cancers characterized by diverse histological subtypes, molecular profiles, and clinical outcomes, especially in women. In this investigation, the development of copper(Cu)-tris((1H-benzo[d]imidazol-2-yl)methyl)amine (NTB) or $[Cu(NTB)(OH_2)](ClO_4)_2$ complex was initiated and further characterized by UV-visible spectroscopy, IR, and ^1H NMR spectroscopy to understand the physicochemical properties of the Cu-NTB complex. The Cu-NTB complex was further explored to determine the anti-cancer effectiveness against MDA-MB-231 TNBC cells and showed an IC_{50} value of 5.60 μg/mL when compared with cisplatin (i.e., 6.95 μg/mL). In addition, the investigation further explored 4 and 8 μg/mL concentrations of Cu-NTB complex treatment in cancer cells to understand the DNA damage and apoptosis via TUNEL assay, Hoechst and PI staining, LysoTracker, and MitoTracker assays. Moreover, the maximum concentration of the Cu-NTB complex, i.e., 8 μg/mL treatment disrupted cellular organelle, which was further confirmed through transmission electron microscopy (TEM). Altogether, this investigation further establishes the potential apoptosis effect of the Cu-NTB complex in MDA-MB-231 TNBC cells; further studies are required to establish the efficacy in preclinical and clinical models.

Abbreviations: BC, breast cancer; Cu, copper; FACS, fluorescence-activated cell sorting; NPs, nanoparticles; NTB, tris((1H-benzo[d]imidazol-2-yl)methyl)amine; ROS, reactive oxygen species; TEM, transmission electron microscopy; TNBC, triple-negative breast cancer; TUNEL, terminal deoxynucleotidyl transferase dUTP nick-end labeling.

This is an open access article under the terms of the Creative Commons Attribution License, which permits use, distribution and reproduction in any medium, provided the original work is properly cited.

© 2025 The Author(s). *Nano Select* published by Wiley-VCH GmbH.

1 | Introduction

Breast cancer (BC) is a devastating disease that poses a significant threat to women's health globally [1]. BC remains one of the most critically diagnosed cancers and the major cause of cancer-related deaths among women across the globe [2]. In 2022, there were an estimated 2.3 million new cases of BC, and 670 000 associated deaths reported [3]. As per the latest report, 15%–20% of all BC cases are triple-negative breast cancer (TNBC), which is characterized by the absence of hormonal receptors (i.e., estrogen and progesterone) along with a lack of expression of human epidermal growth factor receptor 2 (HER2) [4, 5]. Particularly, TNBC emerges as an aggressive and challenging subtype, as the recurrence is higher in this subtype. In addition, the occurrence of metastasis and poor prognosis compared to other BC subtypes make it challenging for clinicians [4, 6]. Despite advancements in early detection or diagonosis and conventional therapies, i.e., surgery, chemotherapy, and radiation therapy, the prognosis of several patients remains poor due to the aggressive nature of TNBC and the severe side effects associated with the conventional interventions [4]. The conventional therapies often lack specificity, leading to significant toxicity to normal cells [7]. Additionally, these are also associated with high mortality rates and increased resistance development, thereby rendering these treatments ineffective over time [8]. This underscores the urgent need to develop novel therapeutic approaches, especially for patients with TNBC, that offer specific, efficient, and targeted treatment options with minimal adverse events.

In recent years, metal-based compounds exhibited or evolved as a new promising approach in cancer management. The metal-based compounds possess distinguished pathological mechanisms and the potential to overcome drug resistance in cancer treatment [9, 10]. Among these, complexes involving benzimidazole derivatives and metal ions have gained attention for their potential pharmacological properties [11]. Benzimidazole, a heterocyclic aromatic organic compound, is structurally similar to purines, which are integral components of DNA [12]. This structural similarity allows benzimidazole derivatives to interact effectively with biological molecules, enhancing their therapeutic potential. The complexes of benzimidazole with various metals, including copper (Cu), have been explored for their anti-cancer properties, offering new therapeutic avenues in cancer research [11, 13].

Cu has been studied extensively for various pharmaceutical applications and anti-cancer mechanisms. Cu plays a vital role in numerous biological processes, including angiogenesis, free radical generation, and the modulation of immune responses. The existing literature demonstrated that the Cu-based complexes exhibited anti-cancer properties via DNA-directed mechanisms [14, 15]. The extent and intensity of interaction with ligands exhibited the anti-cancer properties of these agents. According to several empirical investigations, Cu is toxic because it can go through redox cycles, consequently scavenging ions from enzyme binding sites and resulting in DNA damage. A compound's affinity, specificity, and stability for DNA are increased when it is modified using a ligand scaffold [14, 15]. These substances have the ability to bind to DNA by noncovalent processes, including electrostatic binding, intercalation, and binding to major or minor grooves of DNA. In addition, several studies have implicated the dysregulation of Cu homeostasis in TNBC tumorigenesis and metastasis [14–16]. Cancer cells often exhibit elevated levels of Cu, which can promote cell proliferation, metastasis, and therapeutic resistance, indicating the significance of exploring Cu-targeted therapies as a potential strategy for treating TNBC and other cancers [14, 15]. The Cu-based complexes further demonstrated remarkable abilities in inducing apoptosis, inhibiting angiogenesis, and generating reactive oxygen species (ROS), thus disrupting the cellular processes essential for cancer cell survival and proliferation. However, in cancer therapy, the clinical utility of Cu in its free ionic form is limited due to its potential systemic toxicity and lack of specificity toward cancer cells [14, 16]. To mitigate these issues, Cu is often complexed with organic ligands, such as benzimidazole, which can enhance its specificity and reduce its toxicity.

Despite the potential of Cu-benzimidazole complexes, their efficacy varies significantly across several cancer cell lines [17]. The recent investigations have shown that these complexes exhibited strong anti-proliferative activity against certain cancer types. The Cu-benzimidazole complexes also demonstrated significant efficacy (at IC_{50} concentrations between 8 and 20 μM) against prostate and hepatic cancer cells [18]. However, these complexes shown moderate cytotoxic and anti-proliferative effects on human BC cells, particularly the highly aggressive TNBC subtype (i.e., MDA-MB-231 cells), as compared to the standard chemotherapeutic agent, i.e., cisplatin [19]. Despite the potential of Cu-benzimidazole complexes, these complexes may require further optimization to enhance their efficacy against BC.

Therefore, this investigation hypothesized that the novel Cu complex with a specific ligand, i.e., tris((1H-benzo[d]imidazol-2-yl)methyl)amine (NTB), may offer improved anti-cancer activity against TNBC cells. Although the Cu-NTB complex has been previously reported in the literature, including preliminary anti-cancer properties, there remains a significant gap in the detailed understanding of its mechanistic actions, especially against aggressive BC subtypes (i.e., TNBC). In this study, we extend beyond basic cytotoxicity assessments to systematically investigate the apoptotic mechanisms induced by Cu-NTB in MDA-MB-231 cells. Unlike previous investigations, our approach integrates advanced cellular and subcellular analyses, including TUNEL assay, Hoechst/PI staining, lysosomal and mitochondrial membrane integrity studies, and ultrastructural assessment via transmission electron microscopy (TEM), which together provide a comprehensive understanding of the intracellular behavior and organelle-specific toxicity of the Cu-NTB complex in TNBC cells. Furthermore, the comparative evaluation with standard treatment (i.e., cisplatin) underscores the enhanced potency and multi-targeted activity of Cu-NTB. These insights offer valuable contributions towards repositioning this well-characterized compound within a new therapeutic context and lay the groundwork for in vivo validation in TNBC management.

2 | Methods

2.1 | Reagents and Chemicals

The reagents o-phenylenediamine, nitrilotriacetic acid, methanol, and copper(II) perchlorate hexahydrate were

26884011, 2025, 12, Downloaded from https://onlinelibrary.wiley.com/doi/10.1002/nano.70049 by Chalmers Research - Chalmers University Of Technology , Wiley Online Library on [03/06/2026]. See the Terms and Conditions (https://onlinelibrary.wiley.com/terms-and-conditions) on Wiley Online Library for rules of use; OA articles are governed by the applicable Creative Commons License

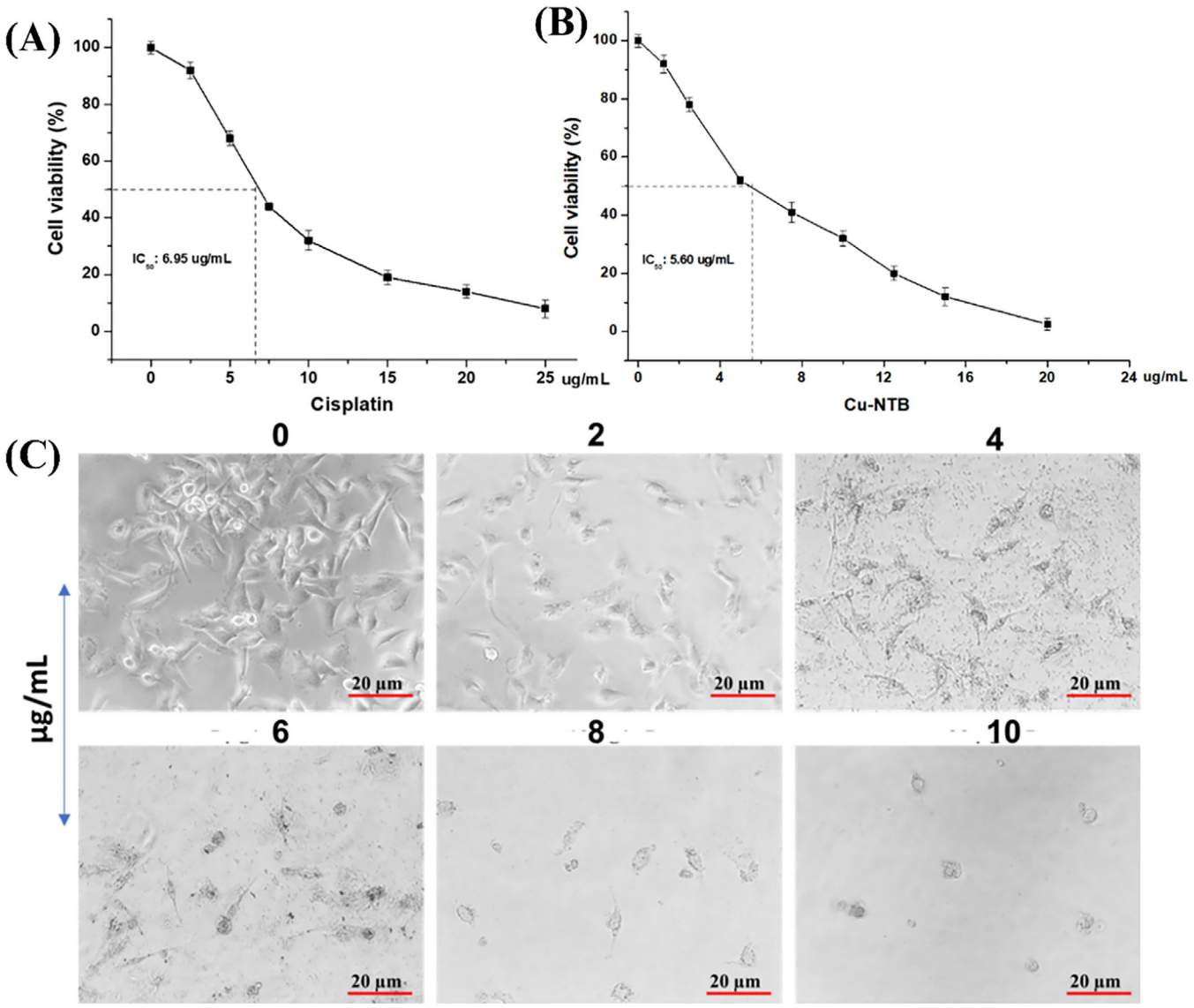

FIGURE 1 | Summary of the IC_{50} concentration determination of (A) Cisplatin (IC_{50} concentration 6.95 µg/mL), and (B) Cu-NTB (IC_{50} concentration 5.60 µg/mL) using MTT assay in MDA-MB-231 cells. (C) Depiction of the morphological characteristic showed in MDA-MB-231 BC cells against Cu-NTB complex induced cell-death in a dose dependent manner between 2 and 10 µg/mL concentrations.

purchased from Sigma-Aldrich, USA. All other chemicals, solvents, and commercial kits used in this study were obtained from standard commercial suppliers and used as received, without further purification. Information regarding the specific kits, including catalog numbers and manufacturers, is provided wherever applicable in the respective experimental sub-sections.

2.2 | Synthesis of Cu-NTB Complex

The ligand NTB was synthesized and reported in previous literature [20, 21]. In brief, o-phenylenediamine (13.5 gm, 125 mmol) and nitrilotriacetic acid (7.65 gm, 40 mmol) were thoroughly mixed, grounded into a fine powder, and heated at 190–200°C for 1 h, using an oil bath. After cooling, the reaction mixture was powdered again, treated with decolorizing charcoal in methanol, and further subjected to hot filtration. Methanol served as the extraction and purification solvent, aiding in the removal of colored and soluble impurities in the synthesis. Upon cooling and solvent evaporation, pink crystals formed, which were collected by filtration and washed with cold methanol to obtain pure NTB compound. The use of methanol at this stage facilitated efficient purification and crystallization of the target complex. The development of the Cu-NTB complex was carried out following a previous study with slight modifications [20, 21]. In addition, Cu (II) perchlorate hexahydrate (0.237 gm, 1 mmol) was dissolved in 10 mL of methanol, and separately, the NTB ligand (0.407 gm, 1 mmol) was dissolved in 20 mL of methanol. The Cu (II) perchlorate hexahydrate solution was then added dropwise to the NTB ligand solution with constant stirring. The resulting mixture was stirred for 1 h, and left to evaporate slowly at room temperature overnight. After adding diethyl ether, the pale green precipitate was collected and dried thoroughly in a vacuum desiccator to remove residual solvent, yielding the final Cu-NTB complex with 76% yield. The product was subsequently subjected to physicochemical, and biological assessments.

26884011, 2025, 12, Downloaded from https://onlinelibrary.wiley.com/doi/10.1002/nano.70049 by Chalmers Research - Chalmers University Of Technology , Wiley Online Library on [03/06/2026]. See the Terms and Conditions (https://onlinelibrary.wiley.com/terms-and-conditions) on Wiley Online Library for rules of use; OA articles are governed by the applicable Creative Commons License

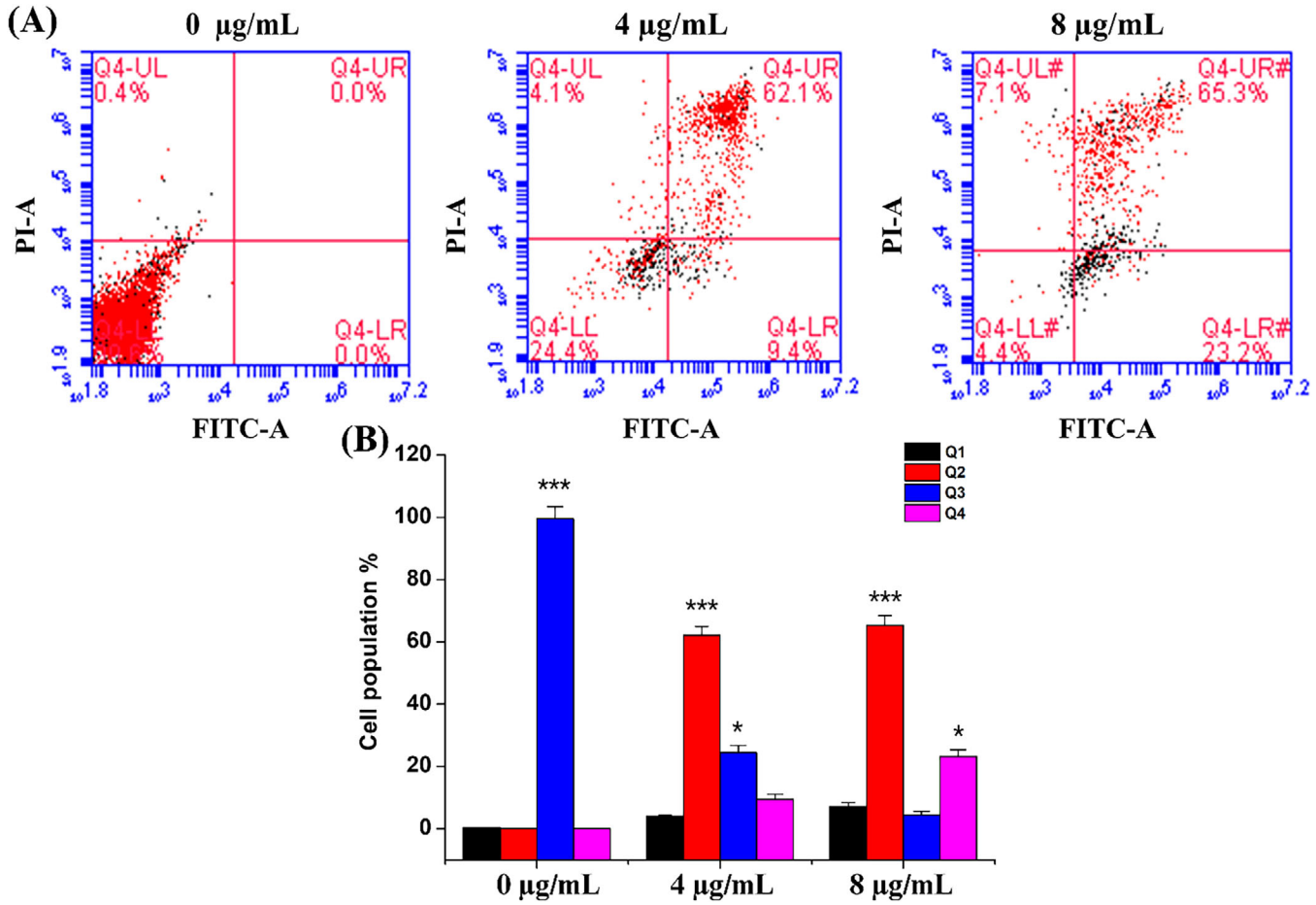

FIGURE 2 | (A) Summary of the FACS analysis in BC cells (MDA-MB-231) treated with 4 and 8 µg/mL of Cu-NTB complex compared to the control (0 µg/mL). Dead cells were stained with PI staining (Red), both live and dead cells were visualized using fluorescence microscopy. (B) Determination of % of cell population at various concentrations of Cu-NTB complex in comparison with control cells. Data are the mean ± SE of three replicates, analyzed using Student's t test. ns, not significant; $^{*}P < 0.05$; $^{**}P < 0.01$; $^{***}P < 0.001$.

2.3 | In Vitro Anti-Cancer Potential of Cu-NTB Complex in MDA-MB-231 Cells

2.3.1 | Cell Culture Condition

The MDA-MB-231 human BC cell line procured from the Korean Cell Line Bank (Seoul, Republic of Korea) was utilized for this study. The cells were maintained in RPMI 1640 medium supplemented with 10% fetal bovine serum (FBS) and 1% antibiotic-antimycotic solution. Cultures were incubated at 37°C in a humidified environment with a 5% CO_2 supply. Cells were routinely passaged to ensure optimal growth, and only healthy, confluent cells were selected for subsequent experimental procedures.

2.3.2 | Determination of Cell Viability

MDA-MB-231 cells (5×10^3 cells/well) were seeded into 96-well plates and allowed to grow for over 24 h, until reaching approximately 80% confluency before treatment. A range of concentrations of Cu-NTB (0 to 25 µg/mL) was prepared to assess the minimum inhibitory concentration against the TNBC cells. Similarly, varying concentrations of the positive control, i.e., cisplatin (0 to 25 µg/mL), were prepared to compare its efficacy with Cu-NTB for further molecular analysis. After 24 h of treatment, both treated and untreated cells were washed twice with 1× PBS (pH 7.4) and then incubated with 100 µL of 0.05% MTT solution for 4 h. Subsequently, the MTT solution was removed, and 200 µL of dimethyl sulfoxide (DMSO) was added to each well. The plates were placed on a rotary shaker to dissolve the purple formazan crystals formed. Untreated cells served as the negative control, while cisplatin was used as the positive control. All experiments were performed in triplicate. The absorbance of the samples was measured at 560 and 670 nm using a VersaMax microplate reader (Molecular Devices, USA).

2.3.3 | Morphological Characteristics of MDA-MB-231 Cells

MDA-MB-231 cells (3×10^4 cells/well) were seeded into 6-well plates for treatment with Cu-NTB and the positive control, i.e., cisplatin, to examine the morphological differences between treated and untreated cells. The control wells received no treatment and displayed normal growth morphology, serving as a

26884011, 2025, 12, Downloaded from https://onlinelibrary.wiley.com/doi/10.1002/nano.70049 by Chalmers Research - Chalmers University Of Technology , Wiley Online Library on [03/06/2026]. See the Terms and Conditions (https://onlinelibrary.wiley.com/terms-and-conditions) on Wiley Online Library for rules of use; OA articles are governed by the applicable Creative Commons License

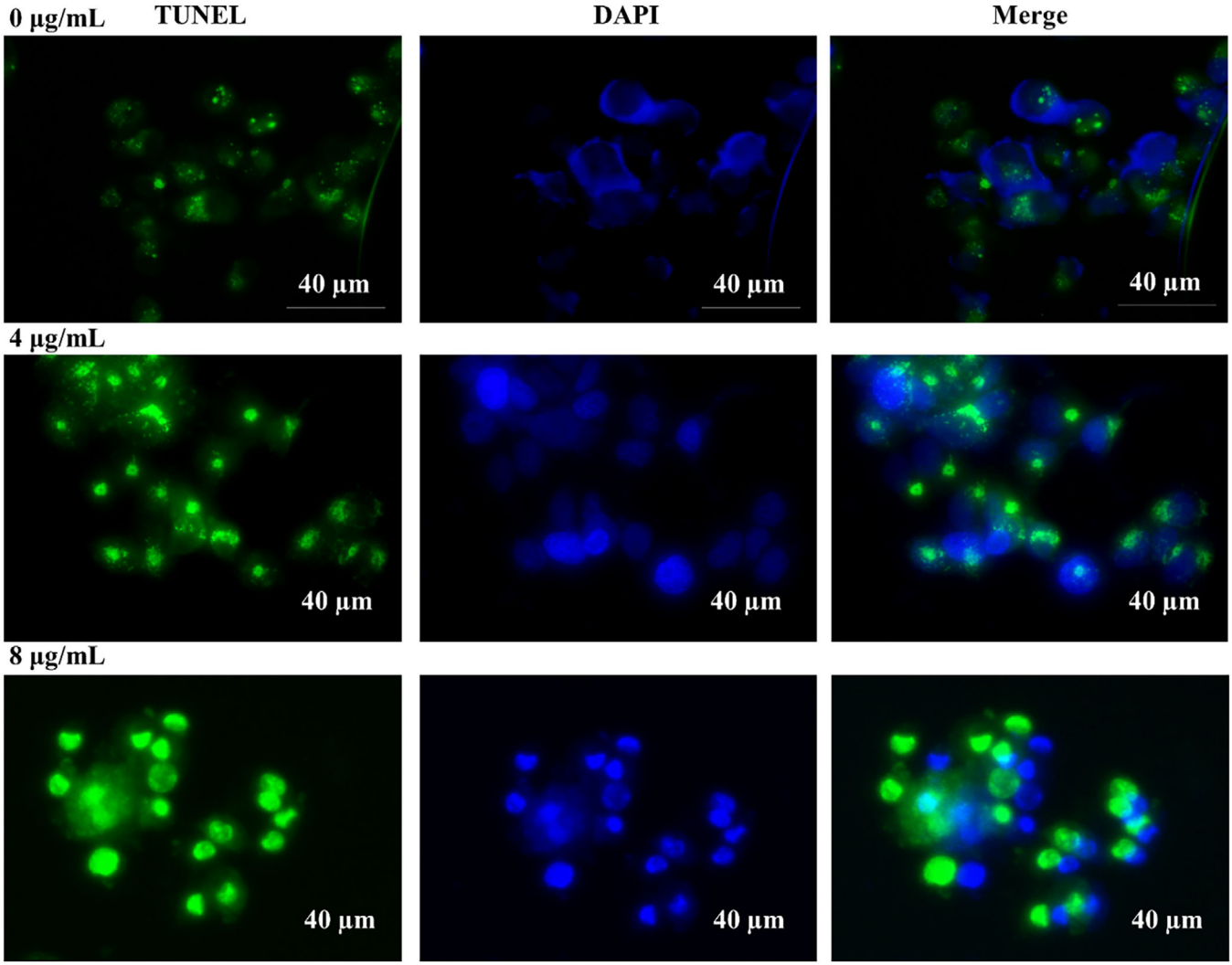

FIGURE 3 | Summary of the early apoptosis of MDA-MB-231 BC cells via DNA fragmentation or damage using Cu-NTB treatment (at 4 and 8 µg/mL concentrations) in merge channel.

reference for comparison with the treated wells. The morphological changes induced by Cu-NTB and cisplatin were analyzed using an inverted light microscope (Leica DMIL LED), allowing for a detailed evaluation of the effects on cellular structure and morphology.

2.3.4 | Fluorescence-Activated Cell Sorting (FACS) via Flow Cytometry

The flow cytometry-mediated FACS analysis was performed using Annexin V/PI staining to evaluate apoptosis-mediated cell death using established protocols. MDA-MB-231 cells (5×10^4 cells/well) were seeded into 6-well plates and incubated until they reached approximately 80% confluency. The cells were then treated with Cu-NTB at two different concentrations (i.e., 4, and 8 µg/mL) for 24 h. Untreated cells were used as controls. After the incubation period, both treated and untreated cells were washed twice with 1x PBS to remove dead cells and debris. The viable cells were carefully detached from the 6-well plates to avoid damage, followed by centrifugation at 1000 rpm for 3 mins. The resulting cell pellets were resuspended in 500 µL of 1x PBS. Samples were prepared with or without Annexin V/PI staining according to the standard protocol and subjected to FACS analysis to quantify apoptotic and viable cell populations.

2.3.5 | Detection of DNA Damage

Terminal deoxynucleotidyl transferase dUTP nick-end labeling (TUNEL) assay was conducted to further confirm Cu-NTB-induced cell death. For this assay, MDA-MB-231 cells (2×10^4 cells/well) were treated with the same two concentrations of Cu-NTB (4 and 8 µg/mL) for 24 h, and staining was performed according to established methods. All experimental groups, including treated and untreated controls, were carried out in triplicate. To assess apoptosis-mediated cell death, various fluorescent staining techniques were employed, including Hoechst and propidium iodide (PI) staining, following previously established protocol. Briefly, MDA-MB-231 cells (2×10^4 cells/well) were seeded into 6-well plates and incubated for over 12 h to ensure proper adhesion and growth. Based on the IC_{50} value, two concentrations of Cu-NTB (4 and 8 µg/mL) were prepared for treatment, with untreated cells serving as a negative control. After 24 h of incubation, the

26884011, 2025, 12, Downloaded from https://onlinelibrary.wiley.com/doi/10.1002/nano.70049 by Chalmers Research - Chalmers University Of Technology , Wiley Online Library on [03/06/2026]. See the Terms and Conditions (https://onlinelibrary.wiley.com/terms-and-conditions) on Wiley Online Library for rules of use; OA articles are governed by the applicable Creative Commons License

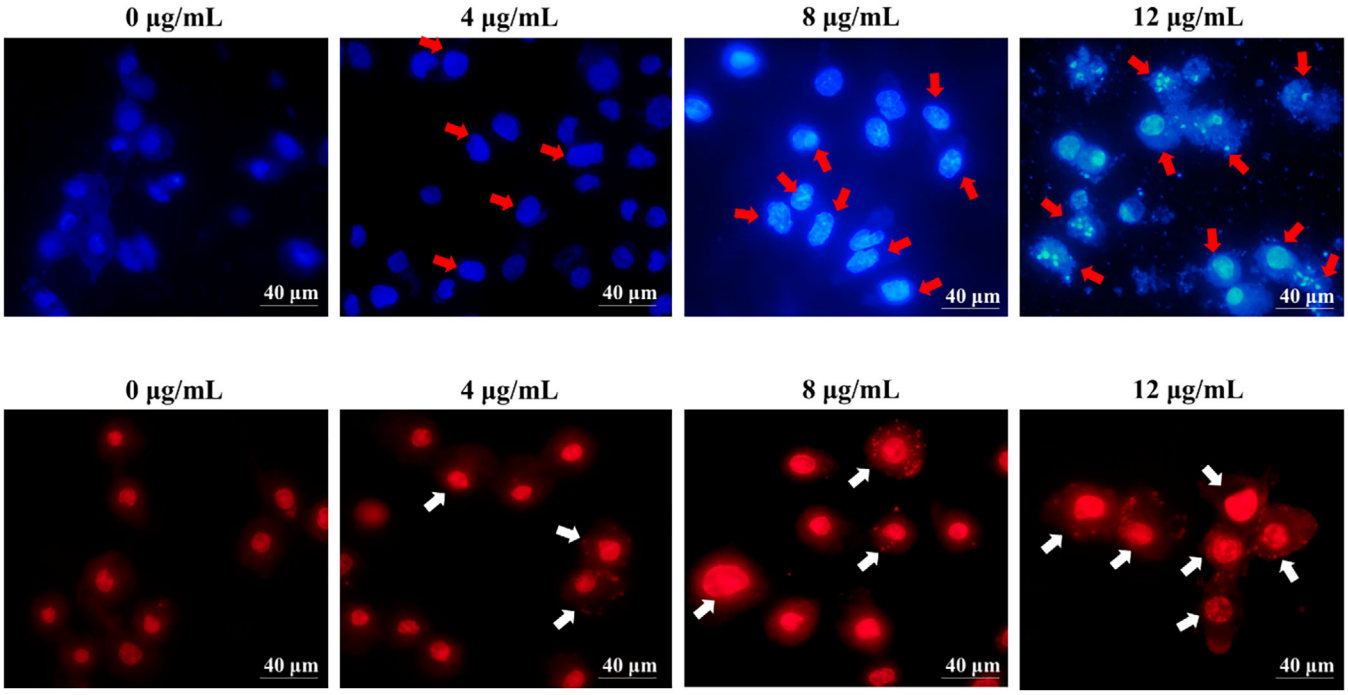

FIGURE 4 | Summary of the Hoechst and PI staining assay results of Cu-NTB complex in BC cells. MDA-MB-231 cells were treated with different concentrations (at 4, 8, and 12 µg/mL) of Cu-NTB complex. Cells that are dead were stained using Hoechst (Blue) and PI (Red) dye to emit fluorescence.

wells were washed twice with 1x PBS to remove dead cells and debris. The cells were then fixed with 4% paraformaldehyde, and Hoechst and PI staining were performed individually as described in the literature [22].

2.3.6 | Lyso/Mito-Tracker Assay

MitoTracker and LysoTracker staining assays were performed to visualize and confirm whether Cu-NTB-induced cytotoxicity involved mitochondrial dysfunction and lysosomal destabilization. The changes in organelle morphology and fluorescence intensity provide insights into apoptosis-related events such as mitochondrial membrane potential loss and lysosomal membrane permeabilization [23]. MDA-MB-231 cells (2×10^5 cells/well) were seeded into 6-well plates and allowed to incubate for 24 h prior to treatment. After incubation, the cells were treated with Cu-NTB at different concentrations (4 and 8 µg/mL), while cisplatin (6.95 µg/mL) was used as a positive control to evaluate and compare the efficacy of Cu-NTB. Untreated cells served as a negative control. Following treatment, the culture plates were washed twice with 1x PBS to remove any dead or damaged cells. The cells were then stained using commercially available kits: MitoTracker Red (Cell Signaling Technology, #9082) and LysoTracker Green (Cell Signaling Technology, #8783). Stained cells were visualized using a phase-contrast microscope to assess the effects of Cu-NTB and cisplatin on mitochondrial and lysosomal activity.

2.3.7 | TEM Analysis

MDA-MB-231 cells (2×10^4 cells/well) were seeded into 6-well plates and incubated overnight to ensure proper attachment and growth. The cells were then treated with or without Cu-NTB (at 8 µg/mL) to investigate its localization within cellular organelles and to assess organelle-specific damage. The TEM was performed following a previously established protocol to visualize the effects of Cu-NTB at the ultrastructural level. After treatment, cells were rinsed twice with 1x PBS to remove debris, detached from the culture surface, and centrifuged at 1000 rpm for 3 mins to collect cell pellets. The pellets were then suspended in 10% glycerin and stored for subsequent TEM sample preparation. The samples for TEM analysis were prepared according to the method described in earlier studies. This allowed detailed visualization of the cellular architecture and damage caused by Cu-NTB.

2.4 | Statistical Analysis

All experiments were conducted in triplicate to ensure reliability and reproducibility of the results. The IC_{50} values were calculated using GraphPad Prism software (version 8). Statistical analyses were performed using SAS 9.13 software (SAS Institute, Cary, NC), enabling robust evaluation of the experimental data.

3 | Results and Discussion

3.1 | Synthesis and Characterization of Cu-NTB Complex

The Cu-NTB or [Cu (NTB)$(OH_2)_2$]$(ClO_4)_2$ complex was synthesized in line of our previous investigations [20, 21] and further summarized the chemical reaction of the Cu-NTB synthesis in Figure S1A. The UV spectrum of Cu-NTB complex dispersed in distilled water exhibited a strong absorption between 330 and

26884011, 2025, 12, Downloaded from https://onlinelibrary.wiley.com/doi/10.1002/nano.70049 by Chalmers Research - Chalmers University Of Technology , Wiley Online Library on [03/06/2026]. See the Terms and Conditions (https://onlinelibrary.wiley.com/terms-and-conditions) on Wiley Online Library for rules of use; OA articles are governed by the applicable Creative Commons License

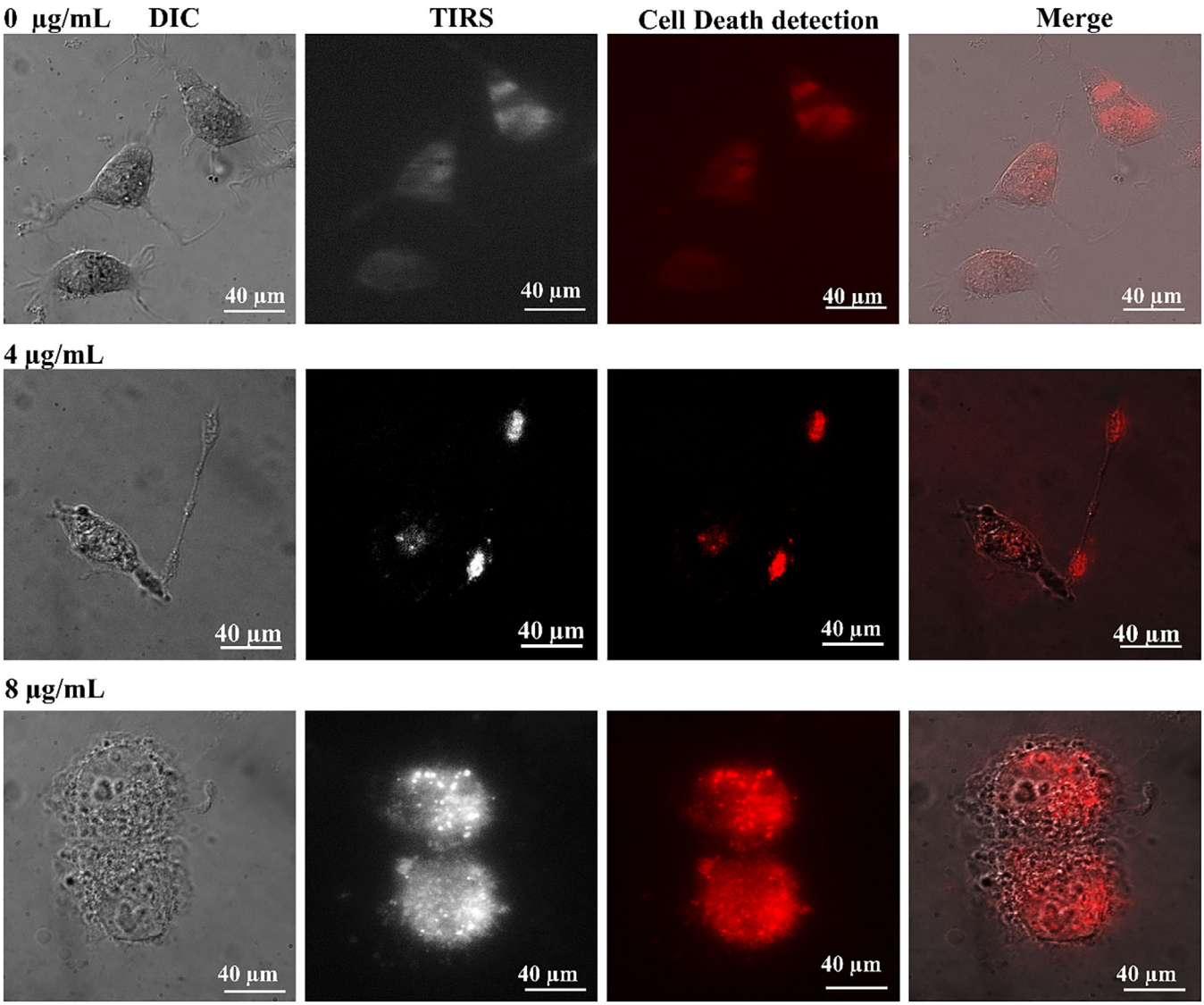

FIGURE 5 | Summary of the detection of apoptotic cells using phase contrast microscopy. MDA-MB-231 cells were treated with 4 and 8 µg/mL of Cu-NTB complex using PI staining to visualize the accumulation of Cu-NTB complex.

350 nm, and another very weak, broad d-d transition between 600 and 950 nm, denoting the formation of Cu (II) complex with NTB (as shown in Figure S1B). The FT-IR spectrum of the Cu–NTB complex confirms the coordination behavior of the NTB ligand with the Cu center. A broad absorption in this region of 3000–3500 cm^{-1} can be attributed to –N–H stretching of secondary amine groups and potentially coordinated water molecules. This suggests the presence of hydrogen bonding or coordinated water within the coordination sphere of the metal. The peaks in the 1400–1600 cm^{-1} region correspond to aromatic C = C and C = N stretching vibrations of the benzimidazole moieties. The presence and shift of the C = N band compared to the free NTB ligand indicates the successful coordination of the nitrogen donor atoms to the Cu^{2+} center [20, 21]. Additionally, a strong band around 1100 cm^{-1} confirms the presence of perchlorate (ClO_4^+) as a counterion (as shown in Figure S1C). The ^1H NMR spectrum of Cu-NTB shows a shift of all the ligand peaks while complexation with Cu atom due to its paramagnetic nature (as shown in Figure S1D). All the changes clearly confirm the complexation of NTB with Cu (II) center, further confirming the formation of the Cu-NTB complex.

3.2 | Cell Viability and Morphological Characteristics

Cu-NTB was investigated for its anti-cancer potential against MDA-MB-231 TNBC cells and compared with a standard anti-cancer drug, i.e., cisplatin. The IC_{50} value of cisplatin was 6.95 µg/mL, which was higher when compared to the IC_{50} value of the Cu-NTB complex, i.e., 5.60 µg/mL against TNBC cells, as shown in Figure 1A,B, respectively. The Cu-NTB complex demonstrated superior cytotoxic efficacy compared to cisplatin, as evidenced by its lower IC_{50} value. There are various studies that indicate the anti-cancer activity of Cu nanoparticles (NPs) against different cancer cell lines. In a recent study, Abdollahzadeh H. et al. reported Cu-based complex with IC_{50} values ranging from 24.59 to 330.8 µg/mL for HEK-293, 27.41 to 128.8 µg/mL for HCT-

26884011, 2025, 12, Downloaded from https://onlinelibrary.wiley.com/doi/10.1002/nano.70049 by Chalmers Research - Chalmers University Of Technology , Wiley Online Library on [03/06/2026]. See the Terms and Conditions (https://onlinelibrary.wiley.com/terms-and-conditions) on Wiley Online Library for rules of use; OA articles are governed by the applicable Creative Commons License

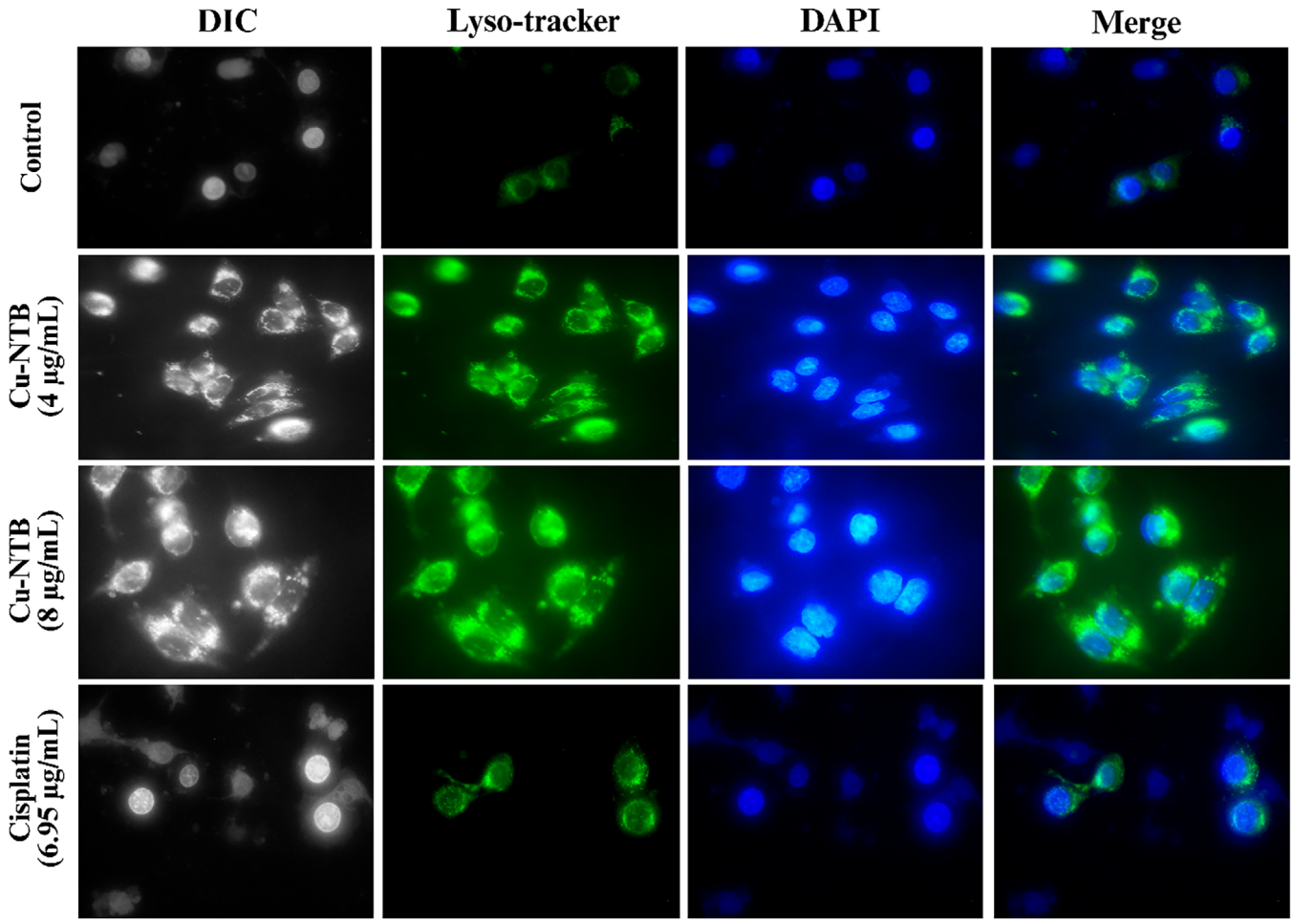

FIGURE 6 | LysoTracker shows apoptosis regions in the treated cells with Cu-NTB complex. Apoptosis induced by 4 and 8 μg/mL of Cu-NTB complex and 6.95 μg/mL of cisplatin (positive control) presented by green color compared to the control (0 μg/mL). Double-stranded DNA is also counterstained by DAPI (in blue color). LysoTracker and DAPI signals were colocalized in merged images. Scale bar = 40 μm.

116, and 28.49 to 221.7 μg/mL for MCF-7 cells [24]. In contrast, the Cu-NTB complex in our study exhibited a significantly lower IC_{50} of 5.60 μg/mL on MDA-MB-231 cells, demonstrating much higher cytotoxic efficacy. In a recent investigation, Foo et al. examined the anti-cancer efficacy of the Cu-based complex, i.e., $Cu(SBCM)_2$ against MCF-7 and non-cancerous MCF-10A breast epithelial cells, reporting IC_{50} values, that is, 32 and 60 μM, respectively, after 48 h, exhibiting selective cytotoxicity toward cancerous cells. The Annexin V-FITC/PI staining further revealed that $Cu(SBCM)_2$ treatment induced both early and late stages of apoptosis in MCF-7 cells, supporting its potential as a promising pro-apoptotic and selective therapeutic agent in BC management [25]. In another investigation, it was demonstrated that the 8-aminoquinoline-naphthyl copper (Cu8AqN) complex effectively inhibited MCF-7 and MDA-MB-231 BC cells, with IC_{50} concentrations of 2.54 ± 0.99 and 3.31 ± 0.12 μM, respectively. This study further confirmed that the complex induced early and late apoptosis in Annexin V/PI staining assay [26]. In a similar context, the Cu(II)-tropolone (trp) [$Cu(trp)_2$] complex also exhibited half of the cell death at 5.2 ± 1.8 μM in MCF-7 cells and 4.0 ± 0.2 μM in MDA-MB-231 cells. The study also reported the MDA-MB-231 cells underwent early and late apoptotic and necrotic population, while MCF-7 cells underwent elevated apoptosis compared to TNBC cells at IC_{50} concentration [27]. The mononuclear Cu(II)-dipyrido[3,2-a:2′,3′-c]phenazine (dppz) complex also exhibited potent cytotoxicity against BC cells. The complex further demonstrated time-dependent activity, with IC_{50} values of 0.65 ± 0.01 μM (24 h) and 0.59 ± 0.01 μM (48 h) in MCF-7 cells and 1.4 ± 0.05 μM (24 h) and 0.96 ± 0.02 μM (48 h) in MDA-MB-231 cells. The literature further concluded the early apoptosis of BC cells via chromatin condensation, binucleation, cytoplasmic vacuolation, and membrane blebbing, along with dot-like chromatin indicative of late apoptosis. A considerable proportion of cells also displayed signs of necrotic death, suggesting a mixed mode of cell death induction [28]. In comparison, the Cu-NTB complex in our study exhibited a superior IC_{50} of 5.60 μg/mL against MDA-MB-231 cells, underscoring its enhanced cytotoxic efficacy and potential as a therapeutic agent in comparison with existing literature and standard treatment, i.e., cisplatin (6.95 μg/mL) in TNBC cells.

These results further highlighted the therapeutic potential of Cu-based complexes, particularly Cu-NTB, in targeting BC cells. The cytotoxicity analysis of Cu-NTB exhibited anti-proliferative activity in a dose-dependent manner, as shown in Figure 1C. These microscopic images revealed noticeable morphological alterations in BC cells following treatment with different concentrations of the Cu-NTB complex. The untreated (at 0 μg/mL) or

26884011, 2025, 12, Downloaded from https://onlinelibrary.wiley.com/doi/10.1002/nano.70049 by Chalmers Research - Chalmers University Of Technology , Wiley Online Library on [03/06/2026]. See the Terms and Conditions (https://onlinelibrary.wiley.com/terms-and-conditions) on Wiley Online Library for rules of use; OA articles are governed by the applicable Creative Commons License

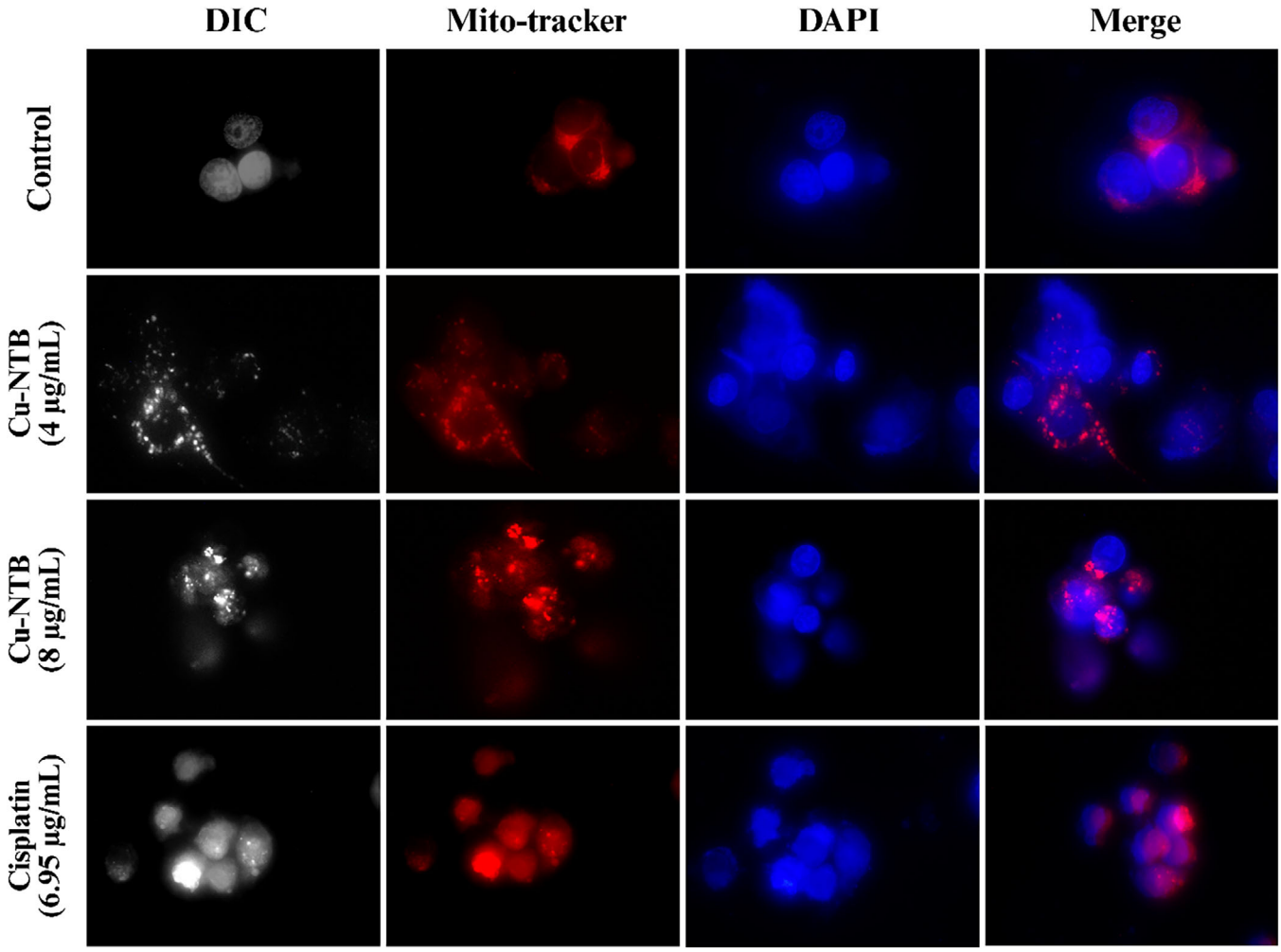

FIGURE 7 | MitoTracker shows apoptosis regions in the treated cells with Cu-NTB complex. Apoptosis induced by 4 and 8 μg/mL Cu-NTB complex as well as 6.95 μg/mL cisplatin (positive control) presented by red color compared to the control (0 μg/mL). Double-stranded DNA is also counterstained by DAPI (in blue color). MitoTracker and DAPI signals were colocalized in merge images. Scale bar = 40 μm.

control cells exhibited typical epithelial morphology with intact cell-cell junctions, indicative of healthy, adherent cells. However, as the concentration of Cu-NTB increased (2–10 μg/mL), cells underwent significant structural changes, including shrinkage, detachment from the surface, and the appearance of membrane blebbing. These changes are hallmarks of apoptotic and necrotic processes, aligning with the observed reduction in cell viability. These findings further validate the cytotoxic effects of Cu-NTB, as demonstrated in the dose-dependent viability assays.

3.3 | FACS Analysis of Synthesized Cu-NTB Complex

The FACS study demonstrated cancer cell growth was inhibited in a concentration-dependent manner, specifically, Cu-NTB complex can inhibit more cancer cells at 8 μg/mL compared to other concentrations. In the control group (0 μg/mL), the majority of cells remain in the live cell quadrant (Q4-LL), indicating intact cell membranes and minimal apoptotic or necrotic activity. However, the treatment with 4 μg/mL of Cu-NTB results in a significant shift, with a marked increase in early apoptotic cells (Q4-LR, 24.4%) and late apoptotic cells (Q4-UR, 62.1%). This highlights the complex's ability to effectively induce apoptosis at moderate concentrations. At 8 μg/mL, a further increase in late apoptotic cells (65.3%) was observed. The shift in cell death mechanisms at higher doses suggested a progression from early apoptosis to late apoptosis and secondary necrosis as the concentration of Cu-NTB increases. The quantitative analysis, supported by bar plots, confirms the significant reduction in live cells and the corresponding rise in dead cells with increasing Cu-NTB concentrations. The ability of Cu-NTB to induce both apoptosis and necrosis underscores its potential as a dual-mechanism therapeutic agent. This behavior is advantageous, particularly for targeting tumors that are resistant to therapies relying solely on apoptosis induction.

By staining cells with DNA-binding dyes, FACS can be used to analyze the cell cycle distribution of a population, identifying cells in different phases (G0/G1, S, G2/M) [29]. Propidium iodide (PI) also is a fluorescent DNA-binding dye that freely penetrates cell membranes of dead or dying cells but is excluded from viable cells [30]. In addition, PI staining (Red) detects early stage of apoptosis, and FITC-A cells represent necrosis at

26884011, 2025, 12, Downloaded from https://onlinelibrary.wiley.com/doi/10.1002/nano.70049 by Chalmers Research - Chalmers University Of Technology , Wiley Online Library on [03/06/2026]. See the Terms and Conditions (https://onlinelibrary.wiley.com/terms-and-conditions) on Wiley Online Library for rules of use; OA articles are governed by the applicable Creative Commons License

higher concentrations [31], as shown in Figure 2A. As shown in Figure 2A, compared to the control, there was an increased number of apoptotic cells caused by 4 and 8 μg/mL of Cu-NTB complex treated to the cells for 24 h. However, the higher concentration of 8 μg/mL Cu-NTB complex induced a greater number of cells undergoing apoptosis, as evidenced by more black color fluorescence, as shown in Figure 2A. Similarly, in the case of PI, a high number of dead cells were found in the samples treated with 4 and 8 μg/mL of Cu-NTB complex, respectively. These results underscore the concentration-dependent cytotoxicity of the Cu-NTB complex and its potential as a powerful therapeutic agent for inducing apoptosis and necrosis in MDA-MB-231 BC cells, as shown in Figure 2B.

3.4 | DNA Damage Detection via TUNEL Assay

Based on the previous analysis, the apoptosis induced by the Cu-NTB complex was further confirmed via TUNEL assay to understand the apoptosis of MDA-MB-231 BC cells due to DNA damage [32]. The MDA-MB-231 BC cells were treated with 4 and 8 μg/mL concentrations of Cu-NTB complex for 24 h, and TUNEL assay was carried out to detect the DNA damage that normally arises during early and late stages of apoptosis, as shown in Figure 3. The double-stranded DNA is also counterstained by DAPI (in blue color) that intercalates between strands of double-stranded DNA [32], as depicted in Figure 3. At 4 μg/mL, the TUNEL signal (green fluorescence) intensifies, indicating an increase in DNA fragmentation. Simultaneously, DAPI staining (blue fluorescence) reveals the presence of condensed and fragmented nuclei, which are characteristic of apoptosis. The merged images demonstrated colocalization of the TUNEL and DAPI signals, further confirming apoptotic activity. This concentration of Cu-NTB effectively induces DNA damage and initiates the apoptotic pathway. At 8 μg/mL, the TUNEL signal becomes more pronounced, reflecting a significant increase in DNA fragmentation. The DAPI staining also shows further nuclear condensation and fragmentation, indicative of advanced stages of apoptosis. The merged images display higher colocalization intensity compared to 4 μg/mL, suggesting that the apoptotic process was more effective at lower concentration.

In addition, the fluorescence intensity histograms confirm a dose-dependent increase in TUNEL (green) and DAPI (blue) signals, with minimal fluorescence in the control group and marked intensities at 4 and 8 μg/mL, indicating enhanced apoptosis. These findings highlight the Cu-NTB complex's potent ability to induce DNA fragmentation and nuclear damage in cancer cells, as shown in the TUNEL graph in Figure 3. The observed increase in DNA fragmentation and nuclear condensation at higher Cu-NTB concentrations is consistent with the mechanisms commonly associated with metal-based complexes. In general, metal-based complexes can generate ROS, including hydroxyl radicals, superoxide anions, and hydrogen peroxide, and can directly attack DNA, leading to the formation of DNA adducts, base modifications (e.g., 8-Oxoguanine), and single- and double-strand breaks [33, 34]. Although studied in different cell lines, Cu-based nanoparticles have also been shown to induce DNA damage via ROS generation, supporting the broader role of copper-mediated oxidative stress in cancer therapy [35, 36]. Additionally, Cu-based compounds can also cause damage to DNA, mitochondria, and cytoplasm due to imbalance in ROS and anti-oxidant systems [37]. In our study, the apoptotic activity highlighted by the TUNEL and DAPI signals at 4 and 8 μg/mL can, therefore, be attributed to the ROS-mediated damage initiated by the Cu-NTB complex. Moreover, the interaction of metal-based complexes with BC cells can trigger an inflammatory response, leading to the release of pro-inflammatory cytokines, which further recruit immune cells such as macrophages and neutrophils [38], which produce additional ROS and reactive nitrogen species (RNS), exacerbating DNA damage [38, 39].

3.5 | Detection of Apoptosis via Hoechst/PI Staining and Phase Contrast Microscopy

The observed results from DAPI staining further supported the potent apoptotic and necrotic effects of the Cu-NTB complex in BC cells. The DAPI results highlight nuclear condensation and fragmentation, indicators of apoptosis. At lower concentrations (4–8 μg/mL), apoptosis was clearly the dominant mechanism, with progressively condensed and fragmented nuclei visible. At the highest concentration tested (12 μg/mL), the degree of nuclear damage escalates, reflecting advanced apoptosis. These changes were mirrored by the fluorescence intensity histograms, which confirm a steady increase in nuclear condensation as the concentration of Cu-NTB rises. Similarly, the PI staining showed the impact of Cu-NTB on cell membrane integrity. While the control group (0 μg/mL) shows negligible PI fluorescence, indicating healthy membranes, higher concentrations reveal increasing disruption of cell membranes. At 4 μg/mL, PI fluorescence indicates the onset of late apoptosis, while 8 μg/mL shows substantial membrane loss, signifying further apoptotic progression. The extensive PI fluorescence at 12 μg/mL highlights a transition to necrosis, likely due to cellular damage.

In our investigation, compared to the control cells, there was an increased number of apoptotic cells caused by different concentrations of Cu-NTB complex (between 4, 8, and 12 μg/mL) for 24 h. However, the higher concentration of 12 μg/mL Cu-NTB complex induced a greater number of cells undergoing apoptosis, as evidenced by more blue color fluorescence, as shown in Figure 4A. In addition, the higher number of dead cells can also be detected in PI staining at 12 μg/mL concentration of Cu-NTB complexes, further supporting the results of Hoechst staining, as shown in Figure 4B. The combination of Hoechst and PI staining in a single experiment allows researchers to simultaneously assess cell viability and nuclear morphology [40]. Hoechst stains all nuclei, but only dead cells take up PI, enabling clear discrimination between live and dead cells, as shown in Figure 4. By assessing chromatin condensation with Hoechst and membrane integrity with PI, the analysis can identify and quantify apoptotic and necrotic cells [31].

In addition, the phase contrast microscopy technique was further utilized to understand the living cells without staining, which can be toxic to cells. It allows real-time observation of dynamic processes such as cell division, motility, and intracellular transport. As shown in Figure 5, the impact of the Cu-NTB complex on MDA-MB-231 cells treated at 4 and 8 μg/mL were visualized

26884011, 2025, 12, Downloaded from https://onlinelibrary.wiley.com/doi/10.1002/nano.70049 by Chalmers Research - Chalmers University Of Technology , Wiley Online Library on [03/06/2026]. See the Terms and Conditions (https://onlinelibrary.wiley.com/terms-and-conditions) on Wiley Online Library for rules of use; OA articles are governed by the applicable Creative Commons License

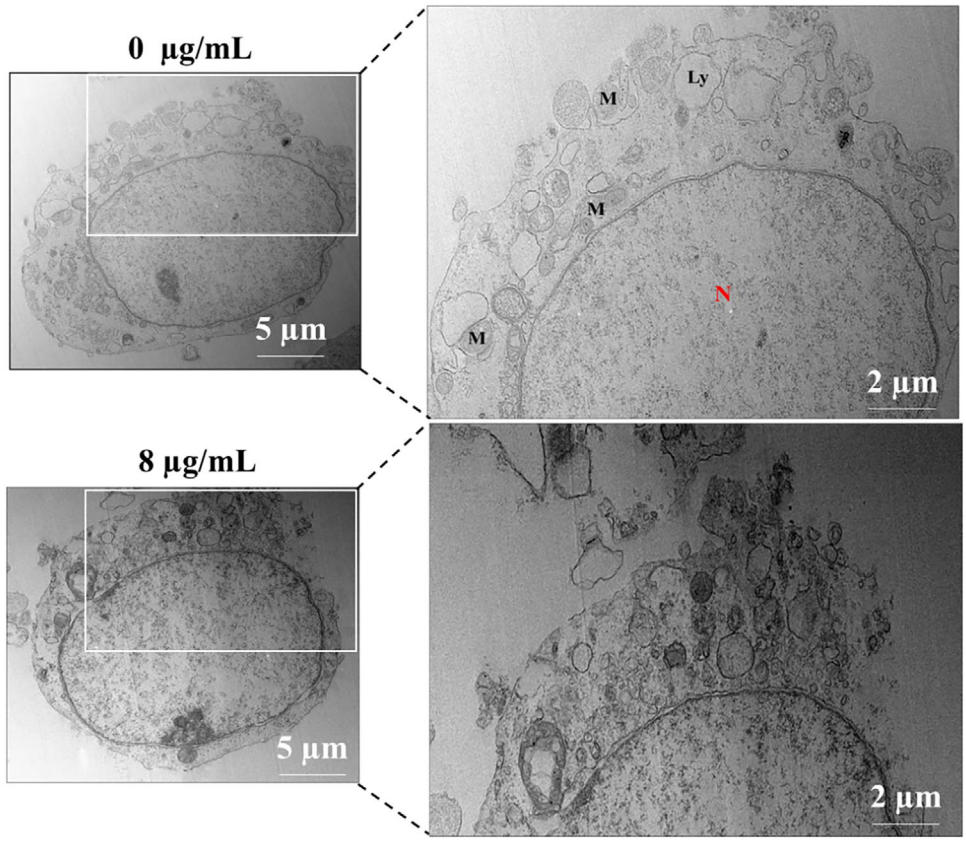

FIGURE 8 | TEM analysis to detect Cu-NTP induced cell death. Apoptosis induced in MDA-MB-231 cells by 8 µg/mL Cu-NTB complex presented by red arrows compared to the control (0 µg/mL).

through phase contrast microscopy and fluorescence staining. In the control group (0 µg/mL), the cells exhibited normal morphology with intact membranes and minimal fluorescence, confirming the absence of cell death. At 4 µg/mL, distinct morphological changes was observed, such as elongation and signs of membrane stress, accompanied by moderate fluorescence, suggesting early stages of cell death. At 8 µg/mL, the effects became more pronounced, with visible cell shrinkage, condensation, and fragmentation. Intense fluorescence was observed at this concentration, indicating significant membrane disruption and advanced cell death. The results highlight a dose-dependent increase in cellular damage and fluorescence intensity, suggesting that Cu-NTB induces apoptosis at lower concentrations and potentially necrotic pathways at higher concentrations.

3.6 | Understanding of Cell Death via LysoTracker, MitoTracker, and TEM

To critically analyze the cell death induced by the Cu-NTB complex at the organelle level, the MDA-MB-231 BC cells were treated with different concentrations of Cu-NTB complex at the concentration range between 4 and 8 µg/mL for 24 h and were further stained with LysoTracker and MitoTracker. The MDA-MB-231 cells treated with cisplatin were used as the positive control. Lysotracker dyes are weakly basic fluorescent probes that selectively label acidic organelles due to protonation. These dyes are fluorescent, allowing for the visualization and tracking of lysosomes using fluorescence microscopy. This staining is particularly useful to look for changes in the overall pattern of apoptosis [41, 42]. The treatment of MDA-MB-231 cells with the Cu-NTB complex at 4 and 8 µg/mL for 24 h induced LysoTracker signal compared to the control samples without any treatment (0 µg/mL), as shown in Figure 6. Double-stranded DNA is also counterstained by DAPI (in blue color). In merged images, LysoTracker-positive puncta appeared where DAPI signals were found, as depicted in Figure 6. In fact, LysoTracker marked the regions of apoptosis that colocalized with double-stranded DNA. Similar to the samples treated with the complex, the treated cells with cisplatin also induced colocalized LysoTracker and DAPI signals, as depicted in Figure 6. The Cu-NTB complex might preferentially accumulate in lysosomes due to its physicochemical properties, such as its charge and size, which favor uptake by acidic organelles [43]. The Cu-NTB complex might induce lysosomal membrane permeabilization, which is often associated with increased LysoTracker signal, as it can lead to changes in lysosomal pH or structure, enhancing dye uptake and retention [44]. In addition, several studies further indicated that the Cu-NTB complex might modulate autophagic processes, leading to an increase in autophagolysosomes, and alter the local chemical environment, affecting dye fluorescence [45, 46].

MitoTracker dyes are fluorescent probes specifically designed to stain mitochondria in live cells. They are widely used in cancer biology to study mitochondrial function, dynamics, and integrity. MitoTracker dyes can help elucidate the role of mitochondria in cancer cell metabolism, apoptosis, and drug resistance. MitoTracker dyes are lipophilic cations that selectively accumulate

26884011, 2025, 12, Downloaded from https://onlinelibrary.wiley.com/doi/10.1002/nano.70049 by Chalmers Research - Chalmers University Of Technology , Wiley Online Library on [03/06/2026]. See the Terms and Conditions (https://onlinelibrary.wiley.com/terms-and-conditions) on Wiley Online Library for rules of use; OA articles are governed by the applicable Creative Commons License

in mitochondria due to the organelle's negative membrane potential. Upon accumulation in mitochondria, MitoTracker dyes exhibit fluorescence, allowing for the visualization and analysis of mitochondrial structure and function. Cancer cells often exhibit altered mitochondrial morphology, such as fragmentation or elongation [47, 48]. There were no MitoTracker signal in the control samples with live cells without any treatment (0 μg/mL), as shown in Figure 7. However, the MitoTracker signal was detected in 4 and 8 μg/mL Cu-NTB complex as well as 6.95 μg/mL of cisplatin, respectively. Double-stranded DNA is also counterstained by DAPI (in blue color), and the MitoTracker and DAPI signals were colocalized, as shown in Figure 7. The Cu-NTB complex may preferentially accumulate in mitochondria due to its physicochemical properties. The complex might have a high affinity for the mitochondrial membrane, influencing mitochondrial potential and increasing MitoTracker dye uptake [49]. The Cu-based complexes are known to catalyze the production of ROS. Some MitoTracker dyes, such as MitoTracker Red CM-H2XRos, are sensitive to the redox state of the mitochondria. In addition, the increased ROS production can enhance the fluorescence signal of these dyes [50]. Conversely, if the Cu-NTB complex causes mitochondrial depolarization, it may initially increase the MitoTracker signal due to dye accumulation, followed by a potential decrease if the depolarization is severe. The Cu-NTB complex might influence mitochondrial dynamics, including fission (fragmentation) and fusion (joining). Thus, the complex might stimulate mitochondrial biogenesis, leading to an increased number of mitochondria and thus a higher MitoTracker signal. Similar to our results, the anti-tumor efficacy of the Cu (II) complex of salicylate phenanthroline induced ROS and promoted apoptosis in HCT116 and SW480 cells [51]. In spite of Cu complex's role in ROS and apoptosis, CuO NPs induced toxicity in lung epithelial cells primarily through ROS-mediated oxidative damage. Our findings suggest that the Cu-NTB complex achieves similar effects but with additional mechanisms, including disruption of cellular organelles (lysosomes and mitochondria) and induction of DNA damage, as observed via TUNEL and other staining assays [35]. Both studies underscore the efficacy of Cu-based NPs, but the Cu-NTB complex demonstrates enhanced specificity and effectiveness in cancer cells, possibly due to its ligand-based design facilitating targeted interactions and cellular uptake. These comparisons further emphasize the potential of Cu-NTB as a next-generation therapeutic agent with unique advantages over conventional CuO NPs.

Besides staining with LysoTracker and MitoTracker, the TEM structural analysis provides detailed insights into cellular organelle damage. In untreated cells (0 μg/mL), the cellular structure appears well-preserved, with clearly visible nuclei (N), lysosomes (Ly), mitochondria (M), and Golgi complexes (GC). At 8 μg/mL, cells treated with Cu-NTB exhibit severe structural disruptions. Swollen and fragmented mitochondria disrupted lysosomes, and extensive vacuolization is evident, reflecting advanced cellular damage, as indicated in Figure 8. These observations align with the fluorescence imaging results, confirming that Cu-NTB induces significant lysosomal and mitochondrial damage. The destruction of these organelles suggests a combined mechanism of apoptosis and necrosis, where organelle dysfunction plays a pivotal role in driving cell death. The TEM data thus provide direct visual evidence of Cu-NTB's cytotoxic effects at the ultrastructural level, further substantiating its potential as an anti-cancer agent. The TEM image showed that 8 μg/mL of Cu-NTB complex treatment disintegrates cell organelles significantly compared to control, as indicated in Figure 8.

Thus, all the studies conducted to understand the effect of Cu-NTB on the MDA-MB-231 BC cell line strongly support the potential of the Cu-NTB complex as an effective anti-cancer agent. The results consistently demonstrate its ability to induce cytotoxic effects through apoptosis, mediated by DNA damage, lysosomal membrane permeabilization, and mitochondrial dysfunction. The dose-dependent cytotoxicity of Cu-NTB is evident through the morphological, biochemical, and structural changes observed in the treated cells, which are comparable or superior to cisplatin, a standard anti-cancer drug. These findings provide a solid foundation for further investigations into the molecular pathways underlying Cu-NTB's activity and its evaluation in in vivo models to establish its therapeutic potential for BC treatment.

4 | Conclusion

This study demonstrates the successful synthesis of the Cu-NTB complex and its significant anti-cancer activity against the MDA-MB-231 BC cell line. The complex exhibited superior cytotoxicity compared to cisplatin, inducing dose-dependent apoptosis and necrosis through mechanisms involving organelle disruption, DNA damage, and ROS generation. The lysosomal membrane permeabilization, mitochondrial dysfunction, and ultrastructural disintegration further highlight its multifaceted mode of action. Though our synthesized Cu-NTB complex showed higher toxicity toward BC cells than cisplatin, cytotoxicity towards normal cells must be elucidated for a better understanding. These findings establish Cu-NTB as a promising candidate for BC therapy, warranting further investigation through in vivo studies to evaluate its therapeutic potential and safety profile.

Acknowledgments

The authors would like to extend their sincere appreciation for funding of this work through the National Research Foundation of Korea (NRF), Grant number: 2020R1A6A1A06046728; Ongoing Research Funding program (ORF-2025-349), King Saud University, Riyadh, Saudi Arabia; NNF Grant number: NNF20CC0035580; and DFF and Thematic Research-Independent green research (2023): 3164-00026A. Sourav Mohanto would like to acknowledge Yenepoya (Deemed to be University), India, for providing the fellowship.

Conflicts of Interest

The authors declare no conflicts of interest.

Data Availability Statement

The corresponding author can provide further information, additional data, or justifications related to the experiments upon request.

Supporting Information

The physicochemical characterization and synthesis scheme for Cu-NTB complex are provided in Figure S1.

26884011, 2025, 12, Downloaded from https://onlinelibrary.wiley.com/doi/10.1002/nano.70049 by Chalmers Research - Chalmers University Of Technology , Wiley Online Library on [03/06/2026]. See the Terms and Conditions (https://onlinelibrary.wiley.com/terms-and-conditions) on Wiley Online Library for rules of use; OA articles are governed by the applicable Creative Commons License

References

1. L. Wilkinson and T. Gathani, "Understanding Breast Cancer as a Global Health Concern," *British Journal of Radiology* 95 (2022): 20211033.

2. R. Ebrahimoghli, M. H. Aghaei, S. Azami-Aghdash, and N. Houssami, "Uptake of Breast Cancer Screening Practices in Low- and Middle-Income Countries: A Systematic Review and Meta-analysis," *JNCI: Journal of the National Cancer Institute* 117 (2025): 29–39.

3. F. Bray, M. Laversanne, H. Sung, et al., "Global Cancer Statistics 2022: GLOBOCAN Estimates of Incidence and Mortality Worldwide for 36 Cancers in 185 Countries," *CA: A Cancer Journal for Clinicians* 74 (2024): 229–263.

4. G. Ioele, M. Chieffallo, M. A. Occhiuzzi, et al., "Anticancer Drugs: Recent Strategies to Improve Stability Profile, Pharmacokinetic and Pharmacodynamic Properties," *Molecules* 27 (2022): 5436.

5. H. Yao, G. He, S. Yan, et al., "Triple-Negative Breast Cancer: Is There a Treatment on the Horizon?" *Oncotarget* 8 (2016): 1913–1924.

6. O. Obidiro, G. Battogtokh, and E. O. Akala, "Triple Negative Breast Cancer Treatment Options and Limitations: Future Outlook," *Pharmaceutics* 15 (2023): 1796.

7. Z. Lei, Q. Tian, Q. Teng, et al., "Understanding and Targeting Resistance Mechanisms in Cancer," *Medical Communications* 4 (2023): e265.

8. M. Arnold, E. Morgan, H. Rumgay, et al., "Current and Future Burden of Breast Cancer: Global Statistics for 2020 and 2040," *Breast* 66 (2022): 15–23.

9. S. Adhikari, P. Nath, A. Das, et al., "A Review on Metal Complexes and Its Anti-Cancer Activities: Recent Updates From In Vivo Studies," *Biomedicine & Pharmacotherapy* 171 (2024): 116211.

10. R. L. Lucaciu, A. C. Hangan, B. Sevastre, and L. S. Oprean, "Metallo-Drugs in Cancer Therapy: Past, Present and Future," *Molecules* 27 (2022): 6485.

11. V. T. Nguyen, T. K. C. Huynh, G. T. T. Ho, et al., "Metal Complexes of Benzimidazole-Derived as Potential Anti-Cancer Agents: Synthesis, Characterization, Combined Experimental and Computational Studies," *Royal Society Open Science* 9 (2022): 220659.

12. K. Mahmood, Z. Akhter, F. Perveen, et al., "Synthesis, DNA Binding and Biological Evaluation of Benzimidazole Schiff Base Ligands and Their Metal (ii) Complexes," *RSC Advances* 13 (2023): 11982–11999.

13. Y. T. Lee, Y. J. Tan, and C. E. Oon, "Benzimidazole and Its Derivatives as Cancer Therapeutics: The Potential Role From Traditional to Precision Medicine," *Acta Pharmaceutica Sinica B* 13 (2023): 478–497.

14. S. Abdolmaleki, A. Aliabadi, and S. Khaksar, "Unveiling the Promising Anticancer Effect of Copper-Based Compounds: A Comprehensive Review," *Journal of Cancer Research and Clinical Oncology* 150 (2024): 213.

15. P. Ji, P. Wang, H. Chen, et al., "Potential of Copper and Copper Compounds for Anticancer Applications," *Pharmaceuticals* 16 (2023): 234.

16. X. Tang, Z. Yan, Y. Miao, et al., "Copper in Cancer: From Limiting Nutrient to Therapeutic Target," *Frontiers in Oncology* 13 (2023): 1209156.

17. D. Yancheva, M. Argirova, I. Georgieva, et al., "Antiproliferative and Pro-Apoptotic Activity and Tubulin Dynamics Modulation of 1 H-Benzimidazol-2-yl Hydrazones in Human Breast Cancer Cell Line MDA-MB-231," *Molecules* 29 (2024): 2400.

18. M. Pellei, C. Santini, L. Bagnarelli, et al., "Exploring the Antitumor Potential of Copper Complexes Based on Ester Derivatives of Bis (Pyrazol-1-yl) Acetate Ligands," *International Journal of Molecular Sciences* 23 (2022): 9397.

19. S. Kacar, H. Unver, and V. Sahinturk, "A Mononuclear Copper (II) Complex Containing Benzimidazole and Pyridyl Ligands: Synthesis, Characterization, and Antiproliferative Activity Against Human Cancer Cells," *Arabian Journal of Chemistry* 13 (2020): 4310–4323.

20. M. Balamurugan, R. Mayilmurugan, E. Suresh, and M. Palaniandavar, "Nickel(ii) Complexes of Tripodal 4N Ligands as Catalysts for Alkane Oxidation Using M-CPBA as Oxidant: Ligand Stereoelectronic Effects on Catalysis," *Dalton Transactions* 40 (2011): 9413, https://doi.org/10.1039/C1DT10902B.

21. S. R. Balusamy, M. Balamurugan, S. Purushothaman, et al., "Apoptotic Cell Death of Stomach Cancer Lines (AGS) Induced by Co-NTB Complex Through Cellular Organelles and DNA Damage," *RSC Advances* 15 (2025): 739–747, https://doi.org/10.1039/D4RA06377E.

22. H. Perumalsamy, K. Sankarapandian, N. Kandaswamy, S. R. Balusamy, D. Periyathambi, and N. Raveendiran, "Cellular Effect of Styrene Substituted Biscoumarin Caused Cellular Apoptosis and Cell Cycle Arrest in Human Breast Cancer Cells," *International Journal of Biochemistry & Cell Biology* 92 (2017): 104–114.

23. B. Zhitomirsky, H. Farber, and Y. G. Assaraf, "LysoTracker and MitoTracker Red Are Transport Substrates of P-Glycoprotein: Implications for Anticancer Drug Design Evading Multidrug Resistance," *Journal of Cellular and Molecular Medicine* 22 (2018): 2131–2141.

24. H. Abdollahzadeh, Y. Pazhang, A. Zamani, and Y. Sharafi, "Green Synthesis of Copper Oxide Nanoparticles Using Walnut Shell and Their Size Dependent Anticancer Effects on Breast and Colorectal Cancer Cell Lines," *Scientific Reports* 14 (2024): 20323.

25. J. B. Foo, L. S. Ng, J. H. Lim, et al., "Induction of Cell Cycle Arrest and Apoptosis by Copper Complex Cu(SBCM)2 Towards Oestrogen-Receptor Positive MCF-7 Breast Cancer Cells," *RSC Advances* 9 (2019): 18359–18370, https://doi.org/10.1039/C9RA03130H.

26. N. Myeza, C. Slabber, O. Q. Munro, et al., "An 8-Aminoquinoline-Naphthyl Copper Complex Causes Apoptotic Cell Death by Modulating the Expression of Apoptotic Regulatory Proteins in Breast Cancer Cells," *European Journal of Pharmacology* 978 (2024): 176764, https://www.sciencedirect.com/science/article/pii/S0014299924004527.

27. L. M. Balsa, M. C. Ruiz, L. Santa Maria de la Parra, E. J. Baran, and I. E. León, "Anticancer and Antimetastatic Activity of Copper(II)-Tropolone Complex Against human Breast Cancer Cells, Breast Multicellular Spheroids and Mammospheres," *Journal of Inorganic Biochemistry* 204 (2020): 110975, https://www.sciencedirect.com/science/article/pii/S0162013419304386.

28. R. Dhivya, P. Jaividhya, A. Riyasdeen, M. Palaniandavar, G. Mathan, and M. A. Akbarsha, "In Vitro Antiproliferative and Apoptosis-Inducing Properties of a Mononuclear Copper(II) Complex With Dppz Ligand, in Two Genotypically Different Breast Cancer Cell Lines," *BioMetals* 28 (2015): 929–943, https://doi.org/10.1007/s10534-015-9877-1.

29. J. P. Robinson, R. Ostafe, S. N. Iyengar, B. Rajwa, and R. Fischer, "Flow Cytometry: The Next Revolution," *Cells* 12 (2023): 1875.

30. M. Rosenberg, N. F. Azevedo, and A. Ivask, "Propidium Iodide Staining Underestimates Viability of Adherent Bacterial Cells," *Scientific Reports* 9 (2019): 6483.

31. D. Wlodkowic, W. Telford, J. Skommer, and Z. Darzynkiewicz, "Apoptosis and Beyond: Cytometry in Studies of Programmed Cell Death," *Methods in Cell Biology* 103 (2011): 55–98.

32. C. Gómez, A. Carreño, D. Ishiwara, et al., "Decatropis Bicolor (Zucc.) Radlk Essential Oil Induces Apoptosis of the MDA-MB-231 Breast Cancer Cell Line," *BMC Complementary and Alternative Medicine* 16 (2016): 266.

33. F. Collin, "Chemical Basis of Reactive Oxygen Species Reactivity and Involvement in Neurodegenerative Diseases," *International Journal of Molecular Sciences* 20 (2019): 2407.

34. C. M. C. Andrés, J. M. P. de la Lastra, C. A. Juan, and F. J. Plou, and E. Pérez-Lebeña, "Chemical Insights Into Oxidative and Nitrative Modifications of DNA," *International Journal of Molecular Sciences* 24 (2023): 15240.

35. H. L. Karlsson, P. Cronholm, J. Gustafsson, and L. Moller, "Copper Oxide Nanoparticles Are Highly Toxic: A Comparison Between Metal Oxide Nanoparticles and Carbon Nanotubes," *Chemical Research in Toxicology* 21 (2008): 1726–1732.

26884011, 2025, 12, Downloaded from https://onlinelibrary.wiley.com/doi/10.1002/nano.70049 by Chalmers Research - Chalmers University Of Technology , Wiley Online Library on [03/06/2026]. See the Terms and Conditions (https://onlinelibrary.wiley.com/terms-and-conditions) on Wiley Online Library for rules of use; OA articles are governed by the applicable Creative Commons License

36. S. Saha, G. Dutta, S. Mohanto, et al., "Sustainable Synthesis of Cr_2O_3 Nanoparticles Utilizing *Rauvolfia tetraphylla* Root Extract for Lung Cancer Treatment," *Journal of Drug Delivery Science and Technology* 104 (2025): 106531, https://www.sciencedirect.com/science/article/pii/S1773224724012000.

37. C. Molinaro, A. Martoriati, L. Pelinski, and K. Cailliau, "Copper Complexes as Anticancer Agents Targeting Topoisomerases I and II," *Cancers* 12 (2020): 2863.

38. R. Yang, L. Chen, Y. Wang, et al., "Tumor Microenvironment Responsive Metal Nanoparticles in Cancer Immunotherapy," *Frontiers in Immunology* 14 (2023): 1237361.

39. O. Habanjar, R. Bingula, C. Decombat, M. Diab-Assaf, F. Caldefie-Chezet, and L. Delort, "Crosstalk of Inflammatory Cytokines Within the Breast Tumor Microenvironment," *International Journal of Molecular Sciences* 24 (2023): 4002.

40. C. Lema, A. Varela-Ramirez, and R. J. Aguilera, "Differential Nuclear Staining Assay for High-Throughput Screening to Identify Cytotoxic Compounds," *Current Opinion in Cell Biochemistry* 1 (2011): 1–14.

41. H. F. G. Barbosa, H. L. Piva, and A. C. Tedesco, "Lysosomal Tracking With Red-Fluorescent Solid Lipid Nanoparticles," *OpenNano* 8 (2022): 100069.

42. S. Chikte, N. Panchal, and G. Warnes, "Use of LysoTracker Dyes: A Flow Cytometric Study of Autophagy," *Cytometry Part A: The Journal of the International Society for Analytical Cytology* 85 (2014): 169–178.

43. R. A. Ndolo, M. L. Forrest, and J. P. Krise, "The Role of Lysosomes in Limiting Drug Toxicity in Mice," *Journal of Pharmacology and Experimental Therapeutics* 333 (2010): 120–128.

44. K. R. Zhang, C. S. R. Jankowski, R. Marshall, et al., "Oxidative Stress Induces Lysosomal Membrane Permeabilization and Ceramide Accumulation in Retinal Pigment Epithelial Cells," *Disease Models and Mechanisms* 16 (2023): dmm050066.

45. Q. Xue, R. Kang, D. J. Klionsky, D. Tang, J. Liu, and X. Chen, "Copper Metabolism in Cell Death and Autophagy," *Autophagy* 19 (2023): 2175–2195.

46. M. A. Rahman, M. S. Rahman, M. A. K. Parvez, and B. Kim, "The Emerging Role of Autophagy as a Target of Environmental Pollutants: An Update on Mechanisms," *Toxics* 11 (2023): 135.

47. K. Neikirk, A. G. Marshall, B. Kula, N. Smith, S. LeBlanc, and A. Hinton, "MitoTracker: A Useful Tool in Need of Better Alternatives," *European Journal of Cell Biology* 102 (2023): 151371.

48. M. I. Sánchez, Y. Vida, E. Pérez-Inestrosa, et al., "MitoBlue as a Tool to Analyze the Mitochondria-Lysosome Communication," *Scientific Reports* 10 (2020): 3528.

49. A. Pedram, M. Razandi, D. C. Wallace, and E. R. Levin, "Functional Estrogen Receptors in the Mitochondria of Breast Cancer Cells," *Molecular Biology of the Cell* 17 (2006): 2125–2137.

50. C. Cottet-Rousselle, X. Ronot, X. Leverve, and J.-F. Mayol, "Cytometric Assessment of Mitochondria Using Fluorescent Probes," *Cytometry Part A* 79A (2011): 405–425.

51. Z. Liu, L. Fan, D. Niu, et al., "Copper (II) Complex of Salicylate Phenanthroline Induces the Apoptosis of Colorectal Cancer Cells, Including Oxaliplatinresistant Cells," *Oncology Reports* 50 (2023): 1–12.

Supporting Information

Additional supporting information can be found online in the Supporting Information section.

Supporting File 1: nano70049-sup-0001-SuppMat.docx.

26884011, 2025, 12, Downloaded from https://onlinelibrary.wiley.com/doi/10.1002/nano.70049 by Chalmers Research - Chalmers University Of Technology , Wiley Online Library on [03/06/2026]. See the Terms and Conditions (https://onlinelibrary.wiley.com/terms-and-conditions) on Wiley Online Library for rules of use; OA articles are governed by the applicable Creative Commons License